Physical Property Estimation and Knife Trajectory Optimization During Robotic Cutting

Xiaoqian Mu and Yan-Bin Jia

***Abstract*— Dexterous robotic cutting needs to demonstrate a skill level with smooth and efficient knife movements. The work performed by the knife mainly generates fracture and overcomes the blade-material friction. This paper presents a recursive least-squares method that repeatedly estimates relevant physical parameters such as Poisson's ratio, fracture toughness, and coefficient of friction, all varying with the knife's movement when cutting a natural food, from force sensor readings. Furthermore, we show that these estimates can be used for generating the knife's trajectory on the fly to either maximize the ease of fracturing or to minimize the rate of work.**

I. Introduction

Cutting of materials especially natural foods is one of many skills that robots have yet to possess. It is an integral part of empowering them to assist people in kitchen and other household tasks. For more than two decades, robotic cutting has been investigated through development of various control strategies [1]–[5]. Meanwhile, research on cutting of biological materials [6] has looked into the roles of blade sharpness and slicing angle [7]–[9]. As of today, machine learning techniques have also been applied to choose the best cutting strategy [10], estimate the "optimal" cutting force [11] and, in addition, control the cutting velocity based on force/torque readings [12].

Theoretical foundation of cutting comes from fracture mechanics [13], [14], in which the work done by the knife is in balance with the total amount of energy required for creating fracture, transformed into other energy forms (strain, kinetic, etc.), and dissipated by friction. Fracture toughness was introduced to quantify the energy spent on propagating a crack by unit area [14, p. 16]. Different explanations [15], [16] were provided for the dramatic decrease in the fracture force when the knife presses and slices the material simultaneously. The phenomenon lacked an in-depth understanding until the recent work [17], in which a stress analysis was offered to show that the value of fracture toughness in a given direction is a fraction of its maximum value (achieved in the vertical direction) and this fraction depends only on the direction as well as the Poisson's ratio of the material.

Dexterous robotic cutting carries the objectives of material separation, smoothness, and efficiency. While the first objective is quite easy to achieve, the last two require some planning and control that make use of material properties, which may be changing as the knife moves through an object. Among these properties, fracture toughness and friction on the blade are the primary affecting factors. For natural foods, both properties vary with the food type, temperature, and degree of freshness, among items of the same type, and even for the same item, with interior layers. Measurement of cutting force and fracture toughness was studied early for ductile materials [18] and live issues [19], [20]. However, these "offline" methods, conducted in advance on other objects of the same type, unrealistically assumed constant property values. The true values for the object being cut may turn out to be quite different.

In this paper, we propose an "online" method that repeatedly estimates three physical parameters: Poisson's ratio ν, fracture toughness R_p, and the product $\tilde{P}$ of the coefficient of friction and average pressure distribution on the knife's blade, all for the specific object as it is being cut open. The method, of recursive least-squares nature, draws upon a recent finding from [17] on the relationship of fracture toughness to the Poisson's ratio and the cutting direction. Section II examines fracture differentially along the curved edge of a translating knife, with a focus on the role of its direction of movement. Section III derives the fracture and frictional forces in terms of the three aforementioned properties, and uses readings from a force/torque sensor as observables to dynamically estimate their changing values.

It is beneficial to adjust the knife's trajectory based the latest parameter estimates so the effort of cutting can be minimized — at least for the moment during the action. Section IV introduces two metrics for planning the knife's next moving direction via minimization. The first metric is the value of fracture toughness while the second one is the amount of total work to yield unit area of fracture. In Section V, experimental results are presented to compare thus generated "optimal" trajectories with straight cutting trajectories. Some discussion and future work are included in Section VI.

In this paper, a vector is represented by a lowercase letter with bold font, e.g, $\boldsymbol{v} = (v_x, v_y)^\top$, with its x- and y- components denoted by the same non-bold letter with subscripts $_x$ and $_y$, respectively. A unit vector carries a hat, for instance $\hat{\boldsymbol{v}} = \boldsymbol{v}/\|\boldsymbol{v}\|$.

*We are grateful to labmate Prajjwal Jamdagni for his valuable feedback and for his discovery of the relationship of fracture toughness to Poisson's and slice/push ratios that made this work possible.

Xiaoqian Mu is with aescape, Brooklyn, NY 11249, USA (xqmu1005@gmail.com). Yan-Bin Jia is with the Department of Computer Science, Iowa State University, Ames, IA 50011, USA (jia@iastate.edu). The work was performed during the first author's Ph.D. study at Iowa State University.

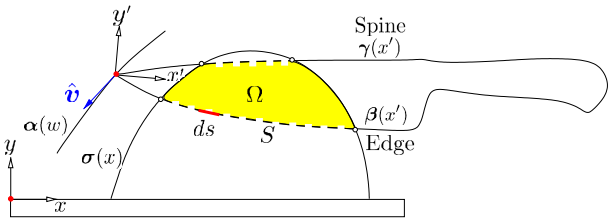

Fig. 1. Geometry of cutting.

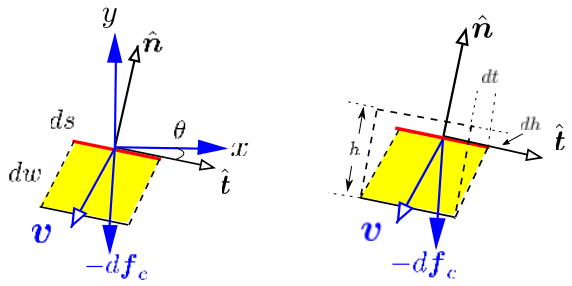

Fig. 2. (a) An element on the knife edge. (b) Local deformable model for the element in (a).

II. Value-Varying Physical Parameters Affecting Fracture

As shown in Fig. 1, cutting takes place in a vertical plane in which the world frame x-y is located at a point on the cutting board. The knife point $\boldsymbol{p}$ moves along a path $\boldsymbol{\alpha}(w)$, possibly generated on the fly, during the action. The path $\boldsymbol{\alpha}(w)$ is represented as a unit-speed curve with w being the arc length. The knife translates throughout cutting. The object's contour in the cutting plane is represented as $\boldsymbol{\sigma}(x) = (x, \sigma(x))^\top$. At the knife point $\boldsymbol{p}$ is a local frame x'-y' in which its spine and edge curves are parameterized in x'.

Two assumptions are made in this paper:

(A1) The object is motionless during cutting.

(A2) As soon as fracture starts, the accumulated strain energy of the object is instantaneously released, restoring the contour $\boldsymbol{\sigma}(x)$ of its cross section in the cutting plane.

The first assumption can be realized by having the object held by a robotic hand or stabilized using a fixture. The second assumption is based on our observations from cutting deformable objects such as eggplants and tomatoes.

During cutting, forces act on the knife's edge and blade by the material of the object. The force $\boldsymbol{f}_c$ exerted on the edge (more accurately, on its portion S inside the object) yields new fracture and is called the cutting force or fracture force. Meanwhile, a frictional force $\boldsymbol{f}_f$ exists in the area Ω of contact between the blade and the material.

A. Fracture by an Infinitesimal Element on the Knife's Edge

Some kitchen knives have straight edges, while others have curved ones. To be general enough, we consider a curved edge with low curvature. Fig. 2(a) shows the interaction between an infinitesimal element on the edge and its vicinity inside the object. Let $\hat{\boldsymbol{n}}$ denote the element's normal direction, $\hat{\boldsymbol{t}}$ its tangential direction, and θ the rotation angle of the local frame $\hat{\boldsymbol{t}}$-$\hat{\boldsymbol{n}}$ from the world frame ($\theta < 0$ in the figure). We consider a movement by the element of an infinitesimal distance dw in the direction

$$\hat{\boldsymbol{v}} = v_t \hat{\boldsymbol{t}} + v_n \hat{\boldsymbol{n}}. \tag{1}$$

Due to the translation, perceived as the movement of the knife point $\boldsymbol{p}$ on the curve $\boldsymbol{\alpha}(w)$, every point on the knife undergoes the same displacement.

The cutting force exerted on this edge element is denoted by $d\boldsymbol{f}_c$. The work done by the element applying the opposite force $-d\boldsymbol{f}_c$ is equal to that for generating the parallelogram of fracture (see Fig. 2(a)):

$$(-d\boldsymbol{f}_c \cdot \hat{\boldsymbol{v}})dw = -R(\hat{\boldsymbol{v}} \cdot \hat{\boldsymbol{n}})dwds, \tag{2}$$

where ds is the arc length of this element, and R the object's *fracture toughness*, which is defined as the energy required to propagate a crack by unit area [14, p. 16].

The cutting force $d\boldsymbol{f}_c$ can be decomposed as

$$d\boldsymbol{f}_c = \begin{pmatrix} df_{cx} \\ df_{cy} \end{pmatrix} = df_{ct}\hat{\boldsymbol{t}} + df_{cn}\hat{\boldsymbol{n}}. \tag{3}$$

Its reaction force $-df_{ct}\hat{\boldsymbol{t}}$ on the object is a shear force with the magnitude

$$-df_{ct} = \frac{G\, dA_f\, dt}{h},$$

where G is the object's shear modulus, dA_f the area that $-d\boldsymbol{f}_c$ acts on, dt the transverse displacement of the element's contact point inside the object, and h the object's original height along $\hat{\boldsymbol{n}}$ (see Fig. 2(b)). Similarly, $-df_{cn}\hat{\boldsymbol{n}}$ is a compression force on the object such that $-df_{cn} = E\, dA_f\, dh/h$, where E is Young's modulus of the object and dh the normal displacement. We assume the object to be isotropic, which gives us $G/E = 1/(2(1+\nu))$, where ν is the Poisson's ratio of the object.

Before crack happens, this element stays with the material right below, yielding a deformation determined by its movement. As a result, the equality $dt/dh = v_t/v_n$ holds. We can represent the ratio between df_{ct} and df_{cn} as follows:

$$\frac{df_{ct}}{df_{cn}} = \frac{1}{2(1+\nu)}\frac{dt}{dh} = \frac{\tilde{\xi}}{2(1+\nu)}, \tag{4}$$

where $\tilde{\xi} = v_t/v_n$ is the *slice-push ratio* of the element's tangential movement to its normal movement.

B. Slice-Push Ratio

Slicing ($v_t \neq 0$) by the knife usually causes less deformation of the object than pressing ($v_t = 0$). This phenomenon is due to a decrease in the fracture toughness under slicing. For an explanation, let us focus on the same element in Fig. 2(a) to see how the fracture toughness varies with the slice-push ratio $\tilde{\xi}$. Recent work [17] derived a ratio between the fracture toughness R_s when the element presses and

slices simultaneously and R_p when it only presses along its normal direction. This ratio assumes the form

$$r = \frac{R_s}{R_p} = \frac{2}{1+\sqrt{1+(\tilde{\xi}/(1-\nu-2\nu^2))^2}}\left(1+\frac{\tilde{\xi}^2}{2(1+\nu)}\right) = \frac{2(1+\nu)+\tilde{\xi}^2}{1+\nu+\sqrt{(1+\nu)^2+(\frac{\tilde{\xi}}{1-2\nu})^2}}. \quad (5)$$

The ratio r can be calculated once ν is known. Till now, the fracture toughness R in (2) can be replaced with the function $R_s(\tilde{\xi},\nu) = rR_p$.

Denote by v_x the x-component of $\hat{\boldsymbol{v}}$ and v_y its y-component. Refer to $\xi = v_x/v_y$ as the slice-push ratio of the knife. We can easily describe the element's slice-push ratio $\tilde{\xi}$ in terms of its local frame:

$$\tilde{\xi}(\xi,\theta) = \frac{v_t}{v_n} = \frac{v_x\cos\theta + v_y\sin\theta}{v_y\cos\theta - v_x\sin\theta} = \frac{\xi+\tan\theta}{1-\xi\tan\theta}. \quad (6)$$

III. Simultaneous Parameter Estimation and Cutting

The Poisson's ratio often varies inside an object. For instance, the central portion of a potato is harder and subjected to less shearing effect than the rest of it. This ratio should therefore be dynamically estimated as cutting proceeds.

The frictional force experienced by the translating knife at its current position can be represented as

$$\boldsymbol{f}_f = -2\mu P\iint_\Omega \hat{\boldsymbol{v}}(x,y)\,dxdy, \quad (7)$$

where μ is the coefficient of friction, P the average pressure distribution over the area Ω of the blade-material contact at the moment. We here introduce a single parameter $\tilde{P} = \mu P$ to further simply the above expression as $\boldsymbol{f}_f = \boldsymbol{f}_f(\tilde{P})$.

Derivation of the overall fracture force is more involved. Along the knife's edge segment S currently inside the object, fracture toughness varies according to (6) depending on the segment's local geometry. In Section III-A, we will derive the fracture force experienced by one element on S, and through integration, obtain the overall fracture force $\boldsymbol{f}_c$.

A. Modeling the Cutting Force

Let us determine the fracture force $d\boldsymbol{f}_c$ on the same element in Fig. 2(a). Substituting (6) into (4), the ratio between the force's tangential and normal components can be rewritten as

$$\frac{df_{ct}}{df_{cn}} = \frac{1}{2(1+\nu)}\,\frac{\xi+\tan\theta}{1-\xi\tan\theta}. \quad (8)$$

The ratio between the two components of the same force in the world frame is

$$\frac{df_{cx}}{df_{cy}} = \frac{df_{ct}\cos\theta - df_{cn}\sin\theta}{df_{cn}\cos\theta + df_{ct}\sin\theta} = \frac{\xi+\tan\theta-2(1+\nu)(1-\xi\tan\theta)\tan\theta}{2(1+\nu)(1-\xi\tan\theta)+(\xi+\tan\theta)\tan\theta} = \frac{c_1\nu+c_2}{c_3\nu+c_4}, \quad (9)$$

where

$$c_1 = -2(1-\xi\tan\theta)\tan\theta,$$
$$c_2 = c_1+\xi+\tan\theta,$$
$$c_3 = -c_1/\tan\theta,$$
$$c_4 = c_3+(\xi+\tan\theta)\tan\theta.$$

Since $\theta < 0$ holds for this element, the above four coefficients are positive as long as ξ is chosen to be positive. The force $d\boldsymbol{f}_c$ exerted on the element thus has the direction

$$\hat{\boldsymbol{e}}_c = \begin{pmatrix} c_1\nu+c_2 \\ c_3\nu+c_4\end{pmatrix}\frac{1}{\sqrt{(c_1\nu+c_2)^2+(c_3\nu+c_4)^2}}. \quad (10)$$

After obtaining $\hat{\boldsymbol{e}}_c$, we can calculate $d\boldsymbol{f}_c$ based on work. Equation (2) balances the work done by $d\boldsymbol{f}_c$ and that for generating a newly fractured area. Here we rewrite it by replacing R with rR_p

$$(-d\boldsymbol{f}_c\cdot\hat{\boldsymbol{v}})dw = -rR_p(\hat{\boldsymbol{v}}\cdot\hat{\boldsymbol{n}})dwds, \quad (11)$$

where, given the knife's slice-push ratio ξ,

$$\hat{\boldsymbol{v}} = \boldsymbol{v}/\|\boldsymbol{v}\| = -\begin{pmatrix}\xi\\1\end{pmatrix}\frac{1}{\sqrt{1+\xi^2}}, \quad (12)$$

r is given in (5), and $\hat{\boldsymbol{n}} = (-\sin\theta,\cos\theta)^\top$. Multiply $\hat{\boldsymbol{e}}_c$ with both sides of the above equation. Cleaning up the resulting equation and observing $d\boldsymbol{f}_c = \|d\boldsymbol{f}_c\|\hat{\boldsymbol{e}}_c$, we arrive at

$$d\boldsymbol{f}_c(\hat{\boldsymbol{e}}_c\cdot\hat{\boldsymbol{v}}) = (rR_p(\hat{\boldsymbol{v}}\cdot\hat{\boldsymbol{n}})ds)\,\hat{\boldsymbol{e}}_c, \quad (13)$$

from which $d\boldsymbol{f}_c$ can be extracted as

$$d\boldsymbol{f}_c = \frac{rR_p(\hat{\boldsymbol{v}}\cdot\hat{\boldsymbol{n}})ds}{\hat{\boldsymbol{e}}_c\cdot\hat{\boldsymbol{v}}}\hat{\boldsymbol{e}}_c = \begin{pmatrix}c_1\nu+c_2\\c_3\nu+c_4\end{pmatrix}\frac{rR_p(-\xi\sin\theta+\cos\theta)ds}{(c_1\nu+c_2)\xi+(c_3\nu+c_4)}. \quad (14)$$

The total cutting force exerted on the knife's edge is subsequently obtained through integration:

$$\boldsymbol{f}_c = \int_S d\boldsymbol{f}_c. \quad (15)$$

By now we have derived the total force $\boldsymbol{f}$ exerted on the knife at the moment:

$$\boldsymbol{f} = \begin{pmatrix}f_x\\f_y\end{pmatrix} = \boldsymbol{f}(\nu,R_p,\tilde{P}) = \boldsymbol{f}_c(\nu,R_p)+\boldsymbol{f}_f(\tilde{P}). \quad (16)$$

B. Estimation using Recursive Least Squares

Denote by $\boldsymbol{x} = (\nu,R_p,\tilde{P})^\top$ the state vector that needs to be estimated. We use the recursive least squares (RLS) filter [21, pp. 84–93] to estimate $\boldsymbol{x}$. The system is described by (16) with its components $\boldsymbol{f}_c$ and $\boldsymbol{f}_f$ given by (15) and (7), respectively. The observation is the reading $\boldsymbol{f}_s = (f_{sx},f_{sy})^\top$ by the force sensor. In the case that any variable in the updated state $\boldsymbol{x}_k$ (obtained from RLS) at the kth step goes out of range, we use the optimization below to bring it back to a value $\boldsymbol{x}_k^*$ within the range:

$$\min\ (\boldsymbol{x}_k^*-\boldsymbol{x}_k)^\top(\boldsymbol{x}_k^*-\boldsymbol{x}_k) \quad (17)$$

subject to constraints:

$$\begin{aligned}(1-\epsilon)f_{sx} \le f_x(\boldsymbol{x}_k^*) \le (1+\epsilon)f_{sx},\\ (1-\epsilon)f_{sy} \le f_y(\boldsymbol{x}_k^*) \le (1+\epsilon)f_{sy},\\ \boldsymbol{l}_{b,k} \le \boldsymbol{x}_k^* \le \boldsymbol{u}_{b,k},\end{aligned}$$

where ϵ is a scalar closer to 0, $\boldsymbol{l}_{b,k}$ is the lower bound, and $\boldsymbol{u}_{b,k}$ is the upper bound.

C. Initialization

At the beginning of cutting, the contact area Ω is negligible, hence the frictional force $\boldsymbol{f}_f \approx \boldsymbol{0}$. This condition, together with assumption A2, implies $\boldsymbol{f}_c \approx \boldsymbol{f}_s$ right after crack begins. Moreover, if the rotation angle θ at each edge element is close to 0, the approximations $df_{cx}/df_{cy} \approx df_{ct}/df_{cn}$ and $\tilde{\xi} \approx \xi$ follow from (9) and (6), respectively. By applying equation (4) and all the approximations mentioned above, we have

$$\frac{f_{sx}}{f_{sy}} \approx \frac{f_{cx}}{f_{cy}} = \frac{\int df_{cx}}{\int df_{cy}} \approx \frac{\xi}{2(1+\nu)}.$$

Thus, we obtain an initial estimate for the Poisson's ratio:

$$\nu_0 \approx \frac{f_{sy}}{2f_{sx}}\xi - 1. \tag{18}$$

IV. Path Planning for Optimal Cutting

The estimation method presented in the previous section works when the knife is simultaneously translating and rotating. This section will focus on the energy optimization for a pure translation by the knife. We will show how to move the knife, at its current position, in a direction that minimizes either fracture toughness or work rate (i.e., the amount of work to fracture unit area). Such a direction, along which the cutting trajectory $\boldsymbol{\alpha}$ will extend, can also be viewed as the curve's tangent. The direction, determined by the slice-push ratio ξ, will allow us to generate $\boldsymbol{\alpha}$ on the fly as the knife moves.

A. Minimum Fracture Toughness

Consider that the knife, at its current position, undergoes an infinitesimal translation specified by its slice-push ratio ξ. The work done by the knife in this movement to create fracture is given as

$$\begin{aligned}dW_c &= \int_S -R_s(\hat{\boldsymbol{v}}\cdot\hat{\boldsymbol{n}})dwds\\ &= R_p\int_S r(\tilde{\xi})\frac{1}{\sqrt{1+\xi^2}}\left(\begin{pmatrix}\xi\\1\end{pmatrix}\cdot\begin{pmatrix}-\sin\theta\\\cos\theta\end{pmatrix}\right)dwds\\ &= R_p\int_S r(\tilde{\xi})\frac{\cos\theta-\xi\sin\theta}{\sqrt{1+\xi^2}}dw\,ds\\ &= \frac{R_p dw}{\sqrt{1+\xi^2}}\int_S r(\tilde{\xi})(\cos\theta-\xi\sin\theta)\,ds,\end{aligned} \tag{19}$$

where $\tilde{\xi}$ can be evaluated according to (6) for each edge element. The new area of crack dA generated by the entire edge can be calculated through integration as follows:

$$\begin{aligned}dA &= -\int_S(\hat{\boldsymbol{v}}\cdot\hat{\boldsymbol{n}})dwds\\ &= \frac{dw}{\sqrt{1+\xi^2}}\int_S(\cos\theta-\xi\sin\theta)ds.\end{aligned} \tag{20}$$

Compared with the definition of fracture toughness, dW_c/dA is viewed as the average fracture toughness over the edge segment S which is performing the cutting at the moment. It has the following form:

$$\frac{dW_c}{dA} = \frac{R_p\int_S r(\tilde{\xi})(\cos\theta-\xi\sin\theta)ds}{\int_S(\cos\theta-\xi\sin\theta)ds}. \tag{21}$$

This toughness measure can achieve a minimum value by picking a slice-push ratio ξ for the current knife position. This ratio, satisfying

$$\frac{\partial(dW_c/dA)}{\partial\xi} = 0, \tag{22}$$

can be found numerically.

When the fracture force dominates the frictional force (as is the case with a potato, apple, etc.), the path generated incrementally by choosing the value of ξ to minimize dW_c/dA is expected to be work-efficient.

B. Minimum Work Rate

It is often necessary to take the work dissipated by friction into consideration when the effect of friction cannot be ignored. In pure translation, the frictional force exerted on the knife's blade has a simple form:

$$\boldsymbol{f}_f = -2\tilde{P}\hat{\boldsymbol{v}} = 2\tilde{P}\Omega\begin{pmatrix}\xi\\1\end{pmatrix}\frac{1}{\sqrt{1+\xi^2}}, \tag{23}$$

where Ω is the knife-object contact area which can be obtained through integration. The work to overcome friction by the blade through an infinitesimal movement dw is

$$dW_f = \|\boldsymbol{f}_f\|dw = 2\tilde{P}\Omega dw. \tag{24}$$

The work dW done by the knife through dw in the direction specified by the ratio ξ is given by $dW = dW_c + dW_f$. The work rate, that is, the work by the knife under the same movement to fracture a unit area, hence is obtained:

$$\frac{dW}{dA} = \frac{R_p\int_S r(\tilde{\xi})(\cos\theta-\xi\sin\theta)ds + 2\tilde{P}\Omega\sqrt{1+\xi^2}}{\int_S(\cos\theta-\xi\sin\theta)ds}. \tag{25}$$

The optimal slice-push ratio satisfies the following equation

$$\frac{\partial(dW/dA)}{\partial\xi} = 0, \tag{26}$$

which can be solved for ξ.

Algorithm 1 summarizes how the parameters are repeatedly estimated during cutting, and how obtained new estimates are immediately used for extending the knife's trajectory. The input of the algorithm is the sensed force $\boldsymbol{f}_s$ and its output is the slice-push ratio ξ.

Algorithm 1 Parameter estimation and trajectory generation

1: Initialize the slice-push ratio ξ
2: After cutting open the object's skin, estimate ν_0 (Section III-C)
3: Set the initial state $\boldsymbol{x}_0 = (\nu_0, 300, 1000)$
4: **repeat**
5: Take the sensor reading $\boldsymbol{f}_{sk}$ at the kth step
6: Update the observation model H_k, covariance R_k of observation noise, Kalman gain K_k, and estimation covariant P_k
7: $\boldsymbol{x}_k = \boldsymbol{x}_{k-1} + K_k(\boldsymbol{f}_{sk} - \boldsymbol{f}(\boldsymbol{x}_k))$
8: **if** $x_{k,i} \geq u_{b,k,i}$ or $x_{k,i} \leq l_{b,k,i}$ $(i = 1, 2, 3)$ **then**
9: Use optimization (17) to regenerate a new state $\boldsymbol{x}_k^*$
10: $\boldsymbol{x}_k = \boldsymbol{x}_k^*$
11: **end if**
12: Optimize the slice-push ratio ξ_k based on $\boldsymbol{x}_k$ (see Section IV)
13: **until** knife contact with the cutting board

V. Experiments

Cutting experiments were preformed with a 4-degrees-of-freedom (4-DOF) WAM Arm which has only two co-planar DOFs. Joints 2 and 4 of the arm were used since joints 1 and 3 did not contribute to the motion in the vertical cutting plane. Mounted on the arm's open end was a 6-axis Delta IP65 F/T sensor from ATI Industrial Automation, to which a kitchen knife was rigidly connected through an adapter.

The knife's edge and spine were modeled in its local x'-y' frame as two quartic polynomial curves $\boldsymbol{\beta}(x')$ and $\boldsymbol{\gamma}(x')$, respectively. A Microsoft Kinect sensor was used to obtain some densely distributed points on the object's surface that were close enough to the cutting plane. These points were then fit over to reconstruct the contour $\boldsymbol{\sigma}(x)$ of the object in the cutting plane containing the world x-y frame.

Due to the robotic arm's lack of one DOF in the cutting plane, the knife could only translate along one circular trajectory. Nevertheless, its rotation in the range of cutting in the experiments was very small compared to its translation, and thus neglected. This allowed us to apply the two trajectory planning methods in Section IV.

We conducted experiments on five types of food items: apple, eggplant, orange, potato, and zucchini.[1] For the purpose of stabilization, half of an object was placed on the cutting board with its flat face down (see Fig. 3). During cutting, the object was constrained by a human hand with some safety measure.

As described in Section III-C, Algorithm 1 generated the initial Poisson's ratio estimate ν_0 roughly after the object's skin was cut open. The moment was determined either from a sudden drop in the vertical component of the sensed force (in the case of a large initial deformation before fracture) or from the calculated fracture area A exceeding certain threshold (in the case of a barely deformable object). The fracture area A is calculated by integrating over the fracture area bounded by $\boldsymbol{\beta}(x')$ and $\boldsymbol{\sigma}(x)$.[2] We found that estimates of ν_0 were reasonable (refer to the common range $[0.0, 0.5]$ of Poisson's ratio) when the knife's slice-push ratio ξ was set close to 1. This value was chosen to initialize ξ in Algorithm 1 for parameter estimation and path planning. To validate the efficiency of a planned path, we compared it against several cutting paths with constant slide-push ratios. These paths were executed on different cross sections of the same object.

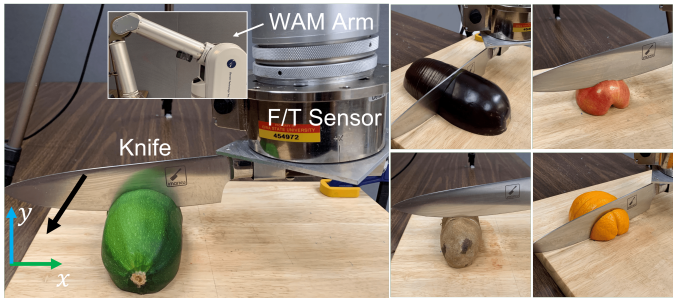

Fig. 3. Experimental setup and five types of objects used in the experiments: zucchini, eggplant, apple, potato, and orange. The black arrow in the setup figure shows the general moving direction of the knife.

Shown in Fig. 4 are the experimental results of cutting an eggplant. Two knife trajectories P_1 and P_2 were first generated to minimize the average fracture toughness dW_c/dA and the work rate dW/dA, respectively. They are respectively colored red and blue in the part (a) of the figure. Cutting was also performed on the same object along five other trajectories with constant slice-push ratios $0.0, 0.5, 1.0, 1.5$, and 2.0 (all plotted in (a)).[3] Shown in (b) are the slice-push ratios along the two trajectories P_1 and P_2. Plotted in (c)–(d) are the two corresponding trajectories of estimates respectively for the Poisson's ratio, and for fracture toughness R_p and the product $\tilde{P}$ of the coefficient of friction and the average pressure distribution. Parameter estimates from the two planned cutting actions were not so close which may have resulted from the seeds inside the eggplant. Shown in (e) are the average fracture toughness W_c/A for the two planned trajectories P_1 and P_2, and other five trajectories shown in (a). It can be seen in (e) that their trajectories resulted in less work per unit area of fracture than the five additional trajectories. In (f), we see that the trajectory with minimum fracture toughness is the most efficient, with savings up to 40% work per unit area compared with other trajectories.

Shown in Fig. 5 are the results from cutting an apple, a potato, an orange, and a zucchini. Except for the apple, the

[1] These natural food items have different level of deformation.

[2] Refer to [5] for more details.

[3] In all the cutting actions, the knife moved along the vertical direction before it contacted the object. That is why the trajectories in (a) are almost vertical at the start.

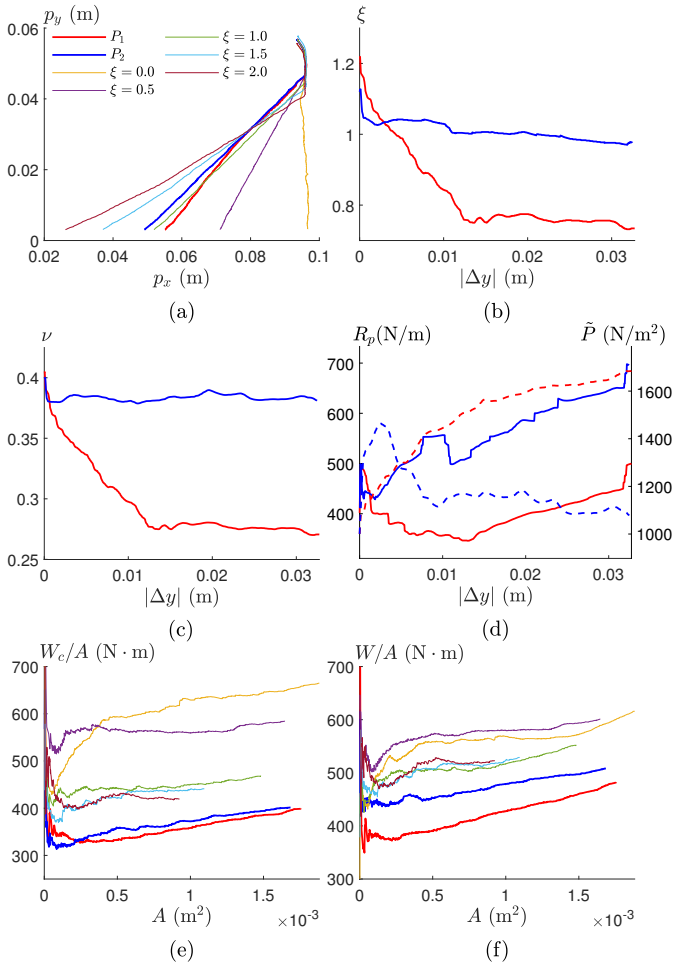

Fig. 4. Cutting an eggplant. (a) Trajectories of minimum fracture toughness and minimum work rate are labeled with P_1 and P_2, respectively, together with five other trajectories with constant slice-push ratios 0, 0.5, 1.0, 1.5, and 2.0. The knife's point $\boldsymbol{p}$ has the position (p_x, p_y). (b) Trajectories of the planned slice-push ratio ξ of P_1 and P_2. (c) Varying estimates of Poisson's ratio ν. (d) Fracture toughness R_p (solid curves, left y-axis), and product $\tilde{P}$ (dashed curves, right y-axis) of the pressure distribution and coefficient of fraction, receptively, from cutting along the paths P_1 and P_2. In these three plots, the x-axis represents the vertical distance traveled by the knife's point. In (e) and (f), the x-axis represents the area A of fracture. (e) Trajectories of W_c/A respectively along the seven trajectories in (a). (f) Trajectories of the work rate W/A.

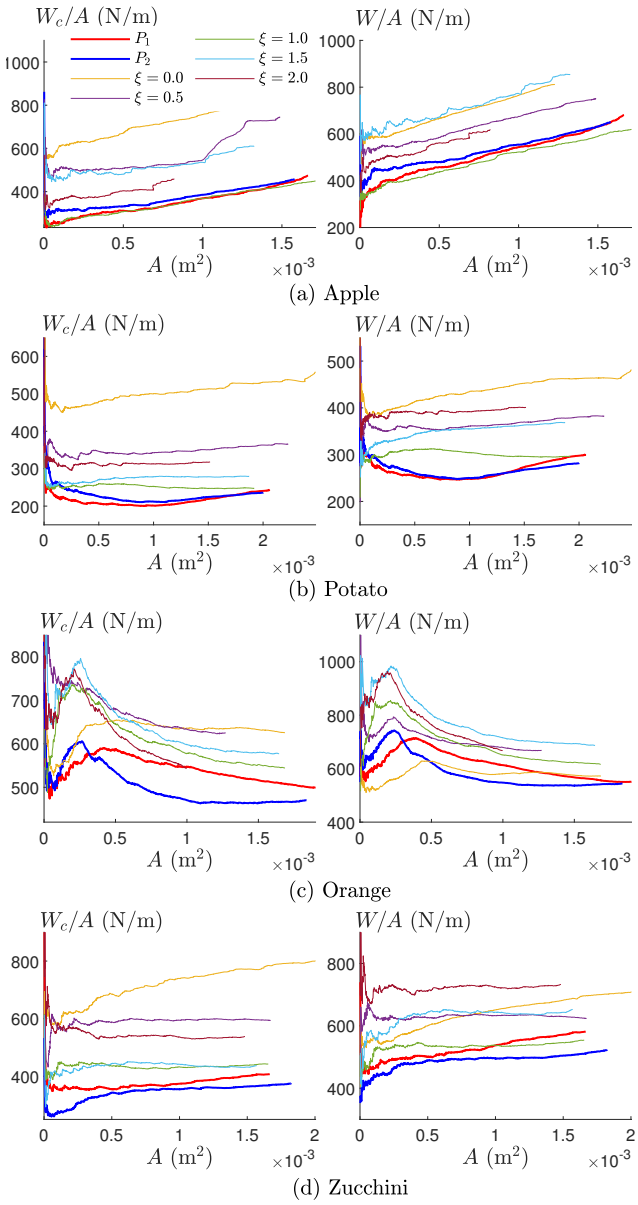

Fig. 5. Outcomes of cutting an an apple, a potato, an orange, and a zucchini.

path P_2 which optimized the work rate claims the minimum W_c/A and W/A at the end of cutting.

In the experiments, we cut more than five individual objects for each of the aforementioned five types. Overall, in more than 90% of all the cutting cases, our planned "optimal" cutting trajectories were more energy efficient than those trajectories with constant slice-push ratios.

VI. Discussion

In this paper, we have presented a method for real-time estimation (and update) of an object's physical parameters including Poisson's ratio, fracture toughness, and a property of friction. With the estimated parameters, knife trajectories under certain optimalities can be generated on the fly by setting a proper slice-push ratio (i.e., the direction of knife movement) at every instant of cutting. Experimental results show that cutting along such planned trajectories work better in most cases than along a path with a constant slice-push ratio.

Since the two introduced trajectory planning methods are based on local optimization, the obtained trajectory might not be optimal for the entire cutting process. Further improvement needs to be investigated, for instance, on the applicability of a more powerful algorithm such as model predictive control (MPC). The introduced path planning method is only for knife translations, despite the applicability of parameter estimation to all motions. An extension to the work-based optimization is to include rotations.

VII. Acknowledgment

The authors would like to thank the anonymous reviewers for their valuable comments.

REFERENCES

[1] G. Zeng and A. Hemami, "An adaptive control strategy for robotic cutting," in *Proc. IEEE Int. Conf. Robot. Autom.*, 1997, pp. 22–27.

[2] S. Jung and T. C. Hsia, "Adaptive force tracking impedance control of robot for cutting nonhomogeneous workpiece," in *Proc. IEEE Int. Conf. Robot. Autom.*, 1999, pp. 1800–1805.

[3] P. Long, W. Khalil, and P. Martinet, "Modeling and control of meat-cutting robotic cell," in *Proc. Int. Conf. Adv. Robot.*, 2013, pp. 61–66.

[4] P. Long, W. Khalil, and P. Martinet, "Force/vision control for robotic cutting of soft materials," in *Proc. IEEE/RSJ Int. Conf. Intell. Robots and Syst.*, 2014, pp. 4716–4721.

[5] X. Mu, Y. Xue, and Y.-B. Jia, "Robotic cutting: Mechanics and control of knife motion," in *Proc. IEEE Int. Conf. Robot. Autom.*, 2019, pp. 3066–3072.

[6] B. Takabi and B. L. Tai, "A review of cutting mechanics and modeling techniques for biological materials," *Medical Eng. Phys.*, vol 45, pp. 1–14, 2017.

[7] D. Zhou and M. R. Claffee, K. M. Lee, and G. V. McMurray, "Cutting, 'by pressing and slicing', applied to the robotic cut of bio-materials. Part I: Modeling of stress distribution," in *Proc. IEEE Int. Conf. Robot. Autom.*, 2006, pp. 2896–2901.

[8] D. Zhou and M. R. Claffee, K. M. Lee, and G. V. McMurray, "Cutting, 'by pressing and slicing', applied to the robotic cut of bio-materials. Part II: Force during slicing and pressing cuts," in *Proc. IEEE Int. Conf. Robot. Autom.*, 2006, pp. 2256–2261.

[9] D. Zhou and G. McMurray, "Modeling of blade sharpness and compression cut of biomaterials," *Robotica*, vol. 28, pp. 311–319, 2010.

[10] Gemici MC and Saxena A (2014) Learning haptic representation for manipulating deformable food objects. In: *Proceedings of the IEEE/RSJ International Conference on Intelligent Robots and Systems*, pp. 638–645.

[11] I. Lenz, R. Knepper, and A. Saxena, "DeepMPC: Learning deep latent features for model predictive control," in *Robot.: Sci. Syst.*, 2015.

[12] I. Mitsioni, Y. Karayiannidis, J. A. Stork, and D. Kragic, "Data-driven model predictive control for the contact-rich task of food cutting," in *Proc. IEEE-RAS Int. Conf. Humanoid Robots.*, 2019, pp. 244–250.

[13] T. L. Anderson, *Fracture Mechanics: Fundamentals and Applications*, 3rd ed., CRC Press, Boca Raton, Florida, 2005.

[14] A. G. Atkins, *The Science and Engineering of Cutting*, Elsevier, Oxford OX2 8DP, UK, 2009.

[15] A. G. Atkins, X. Xu, and G. Jeronimidis, "Cutting, by 'pressing and slicing,' of thin floppy slices of materials illustrated by experiments on cheddar cheese and salami," *J. Mat. Sci.*, vol. 39, pp. 2761–2766, 2004.

[16] E. Reyssat, T. Tallinen, M. Le Merrer, and L. Mahadevan, "Slicing softly with shear," *Phys. Rev. Lett.*, vol. 109, pp. 244301, 2012.

[17] P. Jamdagni and Y.-B. Jia, "Robotic slicing of fruits and vegetables: modeling the effects of fracture toughness and knife geometry," in *Proc. IEEE Int. Conf. Robot. Autom.*, 2021.

[18] T. Atkins, "Toughness and cutting: A new way of simultaneously determining ductile fracture toughtness and strength," *Engr. Fracture Mechanics*, vol. 72, pp. 850-860, 2004.

[19] T. Chanthasopeephan, J. P. Desai, and A. C. W. Lau, "Modeling soft-tissue deformation prior to cutting for surgical simulation: Finite analysis and study of cutting parameters," *IEEE Trans. Biomed. Eng.*, vol. 54, no. 3, pp. 349-=359, 2007.

[20] C. Gokgol, C. Basdogan, D. Canadinc, "Estimation of fracture toughness of liver tissue: Experiments and validation," *Medical Eng. Phys.*, vol. 34, pp. 882—891, 2012.

[21] D. Simon, *Optimal State Estimation*, John Wiley & Sons, Inc., Hoboken, New Jersey, 2006.